

Efficient Hamiltonian engineering

P. Baßler¹, M. Heinrich¹, and M. Kliesch²

¹ Heinrich Heine University Düsseldorf, Faculty of Mathematics and Natural Sciences, Düsseldorf, Germany

² Hamburg University of Technology, Institute for Quantum Inspired and Quantum Optimization, Hamburg, Germany

We propose a novel and efficient scheme to engineer arbitrary (local) many-body Hamiltonians by interleaving the free evolution of a fixed system Hamiltonian with layers of single-qubit Pauli or Clifford gates. These sequences are constructed by solving a linear program (LP) which minimizes the total evolution time. The target Hamiltonians that can be engineered by our method are only limited by the locality of the Pauli terms in the system Hamiltonian. We then construct an efficient relaxation of this LP with a classical runtime that depends on the number of Pauli terms in the Pauli decomposition of the system Hamiltonian and is thus a low-degree polynomial in the number of qubits in practice. With our method, it is also possible to engineer Hamiltonians if only partial knowledge of the system Hamiltonian is available, which can be used to cancel unknown unwanted Pauli terms. We show the classical efficiency of our method by engineering an arbitrary two-body Hamiltonian on a 2D square lattice with 225 qubits in only 60 seconds. We also provide numerical simulations of our method modelling an ion trap device with an Ising Hamiltonian and engineering a general Heisenberg Hamiltonian. Moreover, we address dominant error sources in practical applications.

1 Introduction

Simulating a target Hamiltonian on a quantum system is a central problem in quantum computing, with applications in general gate-based and digital-analog quantum computing, as well as quantum simulations and quantum chemistry [1–6]. It is commonly believed that simulating the dynamics of a quantum system is one of the most promising tasks for showing a practical advantage of quantum computers over classical computers [7], perhaps already in noisy and intermediate scale quantum (NISQ) devices [8, 9]. Especially for the latter, it is essential to have an efficient and fast implementation of the target Hamiltonian due to short coherence times.

The idea to engineer a target Hamiltonian by interleaving the evolution under a fixed system Hamiltonian with single-qubit gates originated in the nuclear magnetic resonance (NMR) community [10–13]. However, previous approaches result in inefficient simulation sequences [10–13], use an inefficient classical pre-processing [14], rely on very specific structures in the system Hamiltonian [15], or require an infinite single-qubit gate set [16–18]. These works are also limited to two-body interactions, and to the best of our knowledge, no general scheme has been developed for many-body interactions. Since there has been an increasing effort in realizing the latter in experiments [19–22], such a general scheme would allow to simulate quantum chemistry Hamiltonians with genuine many-body interactions.

In previous works, we proposed a Hamiltonian engineering method for Ising Hamiltonians based on linear programming and applied it to gate synthesis and compiling problems [23, 24]. In this work, we generalize and extend the linear programming method to efficiently engineer arbitrary target Hamiltonians, which are only limited by the interaction graph of the system Hamiltonian. This target Hamiltonian is simulated using free evolutions under a fixed system Hamiltonian interleaved with Pauli or single-qubit Clifford gates. A crucial feature of our method is that it minimizes

P. Baßler: bassler@hhu.de

M. Kliesch: martin.kliesch@tuhh.de

the total evolution time, leading to a fast implementation of the target Hamiltonian. For larger systems, solving the exact linear program is no longer possible. We thus propose a relaxation that only scales with the number of interaction terms and not directly with the system size, and thus, provides an efficient method to engineer Hamiltonians. This relaxation still yields an exact decomposition of the target Hamiltonian, but the total evolution time is no longer minimal. The latter may, however, be decreased by expanding the search space for the relaxed problem, providing a trade-off between the runtime of the classical pre-processing and the evolution time of the implementation.

2 Preliminaries

We denote by \mathcal{P}^n the set of n -qubit Pauli operators, which can be indexed by binary vectors $\mathbf{a} = (\mathbf{a}_x, \mathbf{a}_z) \in \mathbb{F}_2^{2n}$ such that

$$P_{\mathbf{a}} = P_{(\mathbf{a}_x, \mathbf{a}_z)} = i^{\mathbf{a}_x \cdot \mathbf{a}_z} X(\mathbf{a}_x) Z(\mathbf{a}_z). \quad (1)$$

Here, $X(\mathbf{x}) := X^{x_1} \otimes \cdots \otimes X^{x_n}$ and $Z(\mathbf{z}) := Z^{z_1} \otimes \cdots \otimes Z^{z_n}$ where X, Z are the single-qubit Pauli matrices. Sometimes, we also call $P_{\mathbf{a}}$ a *Pauli string*. They satisfy the following commutator relation

$$P_{\mathbf{a}} P_{\mathbf{b}} = (-1)^{\langle \mathbf{a}, \mathbf{b} \rangle} P_{\mathbf{b}} P_{\mathbf{a}}, \quad (2)$$

for any $\mathbf{a}, \mathbf{b} \in \mathbb{F}_2^{2n}$ with the binary symplectic form on \mathbb{F}_2^{2n} defined by $\langle \mathbf{a}, \mathbf{b} \rangle := \mathbf{a}_x \cdot \mathbf{b}_z + \mathbf{a}_z \cdot \mathbf{b}_x$, where the sum is taken in \mathbb{F}_2 , i.e., modulo 2.

Elements of \mathcal{P}^n form a basis of the complex $2^n \times 2^n$ matrices. Any $H \in \mathbb{C}^{2^n \times 2^n}$ can be written as

$$H = \sum_{\mathbf{a} \in \mathbb{F}_2^{2n}} J_{\mathbf{a}} P_{\mathbf{a}}, \quad (3)$$

with $J_{\mathbf{a}} \in \mathbb{C}$. If H is a Hermitian operator, which we denote by $H \in \text{Herm}(\mathbb{C}^{2^n})$, then $J_{\mathbf{a}} \in \mathbb{R}$. We collect all $J_{\mathbf{a}}$ in a vector $\mathbf{J} \in \mathbb{R}^{4^n}$ with indices $\mathbf{a} \in \mathbb{F}_2^{2n}$. We define the *support* of a Pauli string $P_{\mathbf{a}}$ as $\text{supp}(P_{\mathbf{a}}) := \text{supp}(\mathbf{a}) := \{i \in [n] | a_{x_i} \neq 0 \text{ or } a_{z_i} \neq 0\}$, i.e. the qubit indices where the Pauli string acts on non-trivial. We call

$$H = \sum_{\mathbf{a} \in \mathbb{F}_2^{2n}} J_{\mathbf{a}} P_{\mathbf{a}}. \quad (4)$$

k -local if $J_{\mathbf{a}} = 0$ whenever $|\text{supp}(\mathbf{a})| > k$.

3 Hamiltonian engineering

We wish to implement the time evolution of a *target Hamiltonian* H_T by having access to some simple gates (e.g., certain single-qubit gates) plus the time evolution under some *system Hamiltonian* H_S . The system Hamiltonian can be an arbitrary Hamiltonian that is native to the considered quantum platform. That is, we wish to change H_S to achieve an effective Hamiltonian H_T . To this end, we write H_S and H_T in their Pauli decompositions

$$H_S = \sum_{\mathbf{a} \in \mathbb{F}_2^{2n} \setminus \{\mathbf{0}\}} J_{\mathbf{a}} P_{\mathbf{a}}, \quad H_T = \sum_{\mathbf{a} \in \mathbb{F}_2^{2n} \setminus \{\mathbf{0}\}} A_{\mathbf{a}} P_{\mathbf{a}}, \quad (5)$$

with $J_{\mathbf{a}}, A_{\mathbf{a}} \in \mathbb{R}$. We exclude the term $P_{\mathbf{0}} = P_{(0, \dots, 0)} = I^{\otimes n}$, leading to a global and thus unobservable phase. First, we note that the time evolution $e^{-itU^\dagger H U}$ under a Hamiltonian H conjugated by a unitary U can be implemented as $e^{-itU^\dagger H U} = U^\dagger e^{-itH} U$. Now, we want to simulate the time evolution under H_T with H_S by computing a decomposition of the form

$$H_T = \sum_i \lambda_i \mathbf{S}_i^\dagger H_S \mathbf{S}_i, \quad (6)$$

with $\lambda_i > 0$ and $\mathbf{S}_i = S_i^{(1)} \otimes \cdots \otimes S_i^{(n)}$ representing a layer of single-qubit gates, which we later set to be either Pauli or Clifford gates. The time evolution under this decomposition can be

implemented by the time evolution under H_S interleaved with layers of single-qubit gates. Indeed, if all terms in eq. (6) mutually commute, then H_T can be implemented exactly by applying the layer of single-qubit gates \mathbf{S}_1 at time $t = 0$, and then $\mathbf{S}_i \mathbf{S}_{i-1}^\dagger$ at time $\sum_{j=1}^{i-1} \lambda_j$ for $i \geq 1$. In this way, the time evolution under Hamiltonians $\mathbf{S}_i^\dagger H_S \mathbf{S}_i$ is effectively implemented for consecutive times λ_i with $i = 1, 2, \dots$ and leads to the overall time evolution under H_T . If the terms in eq. (6) do not commute, then the time evolution under H_T can be approximated in a similar fashion as for the commuting terms, utilizing suitable Hamiltonian simulation methods (e.g. product formulas).

We introduce the general Hamiltonian engineering method based on linear programming. The effect of $H_S \mapsto \mathbf{S}_i^\dagger H_S \mathbf{S}_i$ on the Pauli coefficients \mathbf{J}_a can be captured by a column vector $W_i \in \mathbb{R}^r$ with elements

$$W_{a,i} = \frac{1}{2^n} \text{Tr} \left(P_a \left(\mathbf{S}_i^\dagger H_S \mathbf{S}_i \right) \right) \quad (7)$$

where r is the number of Pauli terms $\{P_a\}$ we can generate from the ones in H_S by any \mathbf{S}_i . Let s be the number of possible single-qubit layers on n qubits, and define the matrix $W \in \mathbb{R}^{r \times s}$ by taking all vectors W_i as columns. Then, a decomposition (6) can be found by solving the following linear program (LP) minimizing the total evolution time:

$$\begin{aligned} & \text{minimize} \quad \mathbf{1}^T \boldsymbol{\lambda} \\ & \text{subject to} \quad W \boldsymbol{\lambda} = \mathbf{A}, \quad \boldsymbol{\lambda} \in \mathbb{R}_{\geq 0}^s, \end{aligned} \quad (\text{LP})$$

where $\mathbf{1} = (1, 1, \dots, 1)$ is the all-ones vector such that $\mathbf{1}^T \boldsymbol{\lambda} = \sum_i \lambda_i$ and $\mathbf{A} \in \mathbb{R}^r$ represents the Pauli coefficients of the target Hamiltonian H_T . Conjugation of H_S with arbitrary single-qubit gates yields a r which is limited by the locality of the Pauli terms.

(LP) is the main optimization for Hamiltonian engineering and plays a central role in this work. In the following, we discuss basic notations and properties from the theory of linear (and more generally convex) programming [25]. *Feasible solutions* $\boldsymbol{\lambda}$ satisfy all constraints of (LP). An *optimal solution* is a feasible solution that also minimizes the objective function and is indicated by an asterisk as $\boldsymbol{\lambda}^*$. If (LP) has a feasible solution, then there also exists a r -sparse optimal solution $\boldsymbol{\lambda}^*$ [26], corresponding to a decomposition as in eq. (6) with only r terms. Such a r -sparse optimal solution can be found using the simplex algorithm which, in practice, has a runtime that scales polynomially in the problem size $r \times s$ [27]. The main contribution of our work is a hierarchy of relaxations of (LP) with drastically reduced size that still allow for an exact decomposition as in eq. (6).

We now provide general sufficient conditions on the matrix W such that (LP) has a feasible solution for any $\mathbf{A} \in \mathbb{R}^r$.

Definition 3.1. *We say that a matrix $W \in \mathbb{R}^{r \times s}$ is feasible if for each $\mathbf{A} \in \mathbb{R}^r$ there exists a $\boldsymbol{\lambda} \in \mathbb{R}_{\geq 0}^s$ such that $W \boldsymbol{\lambda} = \mathbf{A}$.*

This definition captures the constraints in (LP). An equivalent formulation of W being feasible is that the convex cone generated by the columns of W span \mathbb{R}^r : $\text{cone}(\text{col}(W)) = \mathbb{R}^r$. We will use two well-known results in convex analysis.

Lemma 3.2 (Farkas [28]). *Let $W \in \mathbb{R}^{r \times s}$ and $\mathbf{A} \in \mathbb{R}^r$. Then exactly one of the following assertions is true:*

1. $\exists \mathbf{x} \in \mathbb{R}^s$ such that $W \mathbf{x} = \mathbf{A}$ and $\mathbf{x} \geq \mathbf{0}$.
2. $\exists \mathbf{y} \in \mathbb{R}^r$ such that $W^T \mathbf{y} \geq \mathbf{0}$ and $\mathbf{A}^T \mathbf{y} < \mathbf{0}$.

Lemma 3.3 (Stiemke [29]). *Let $W \in \mathbb{R}^{r \times s}$. Then exactly one of the following assertions is true:*

1. $\exists \mathbf{x} \in \mathbb{R}^s$ such that $W \mathbf{x} = \mathbf{0}$ and $\mathbf{x} > \mathbf{0}$.
2. $\exists \mathbf{y} \in \mathbb{R}^r$ such that $W^T \mathbf{y} \gneq \mathbf{0}$.

With these two lemmas, we can provide a simpler formulation of the feasibility condition on the matrix W .

Proposition 3.4. *Let $W \in \mathbb{R}^{r \times s}$ such that $\ker(W^T) = \{\mathbf{0}\}$. If there exists $\mathbf{x} \in \mathbb{R}^s$ such that $W\mathbf{x} = \mathbf{0}$ and $\mathbf{x} > \mathbf{0}$, then for any $\mathbf{A} \in \mathbb{R}^r$ there exists $\mathbf{x}' \in \mathbb{R}^s$ such that $W\mathbf{x}' = \mathbf{A}$ and $\mathbf{x}' \geq \mathbf{0}$.*

Proof. We show that the second assertion of Farkas lemma is not possible. By lemma 3.3, there does not exist a \mathbf{y} such that $W^T\mathbf{y} \geq \mathbf{0}$. From $\ker(W^T) = \{\mathbf{0}\}$ it follows that if $W^T\mathbf{y} = \mathbf{0}$, then $\mathbf{y} = \mathbf{0}$ which contradicts $\mathbf{A}^T\mathbf{y} < \mathbf{0}$ in the second assertion of lemma 3.2. Finally, the case $W^T\mathbf{y} < \mathbf{0}$ directly contradicts the second assertion of lemma 3.2. \square

To provide a geometric interpretation of proposition 3.4 we first define the *convex hull of the column vectors of W*

$$\text{conv}(W) := \left\{ \mathbf{u} \in \mathbb{R}^r \mid W\mathbf{x} = \mathbf{u}, \mathbf{x} \geq \mathbf{0}, \sum_i x_i = 1 \right\}, \quad (8)$$

and the *interior of a polytope P*

$$\text{int}(P) := \{ \mathbf{u} \in P \mid \exists \varepsilon > 0 \text{ s.t. } \|\mathbf{u} - \mathbf{x}\| < \varepsilon \forall \mathbf{x} \in \mathbb{R}^r \implies \mathbf{x} \in P \}. \quad (9)$$

(LP) is feasible if the convex hull of the column vectors of W has an interior that contains the origin, $\mathbf{0} \in \text{int}(\text{conv}(W))$. The conditions of proposition 3.4 can be efficiently verified: If the LP

$$\begin{aligned} & \text{minimize} && \mathbf{1}^T \mathbf{x} \\ & \text{subject to} && W\mathbf{x} = \mathbf{0}, \\ & && \mathbf{x} \geq \mathbf{1} \end{aligned} \quad (10)$$

has a feasible solution and W has full rank, then W is feasible. Note that proposition 3.4 applies to general matrices and will be useful for the efficient relaxations.

3.1 Pauli conjugation

Conjugation of a system Hamiltonian H_S with a Pauli string $P_{\mathbf{b}}$ leads to

$$P_{\mathbf{b}}^\dagger H_S P_{\mathbf{b}} = \sum_{\mathbf{a} \in \mathbb{F}_2^{2n} \setminus \{\mathbf{0}\}} (-1)^{\langle \mathbf{a}, \mathbf{b} \rangle} J_{\mathbf{a}} P_{\mathbf{a}}, \quad (11)$$

which follows from the commutation relations (2). We want to find a decomposition of H_T with coefficients $\lambda_{\mathbf{b}} \geq 0$ such that

$$H_T = \sum_{\mathbf{a} \in \mathbb{F}_2^{2n} \setminus \{\mathbf{0}\}} A_{\mathbf{a}} P_{\mathbf{a}} = \sum_{\mathbf{b} \in \mathbb{F}_2^{2n}} \lambda_{\mathbf{b}} P_{\mathbf{b}}^\dagger H_S P_{\mathbf{b}}. \quad (12)$$

A $4^n \times 4^n$ matrix with entries $(-1)^{\langle \mathbf{a}, \mathbf{b} \rangle}$ is called a *Walsh-Hadamard matrix*. We define a submatrix $W^{(r \times s)} \in \{-1, 1\}^{r \times s}$ of the Walsh-Hadamard matrix with entries $W_{\mathbf{a}\mathbf{b}}^{(r \times s)} = (-1)^{\langle \mathbf{a}, \mathbf{b} \rangle}$ for d row-indices $\mathbf{a} \in \mathbb{F}_2^{2n}$ and r column-indices $\mathbf{b} \in \mathbb{F}_2^{2n}$. We call $W^{(r \times s)}$ a *partial Walsh-Hadamard matrix*. The dimensions of the partial Walsh-Hadamard matrix are kept visible in our notation since r and s will be parameters in the subsequent sections. In terms of the partial Walsh-Hadamard matrix $W^{((4^n-1) \times 4^n)}$, obtained by omitting the first row corresponding to the identity Pauli term $P_{\mathbf{0}} = I^{\otimes n}$, it follows that

$$H_T = \sum_{\mathbf{a} \in \mathbb{F}_2^{2n} \setminus \{\mathbf{0}\}} \sum_{\mathbf{b} \in \mathbb{F}_2^{2n}} \lambda_{\mathbf{b}} W_{\mathbf{a}\mathbf{b}}^{((4^n-1) \times 4^n)} J_{\mathbf{a}} P_{\mathbf{a}}. \quad (13)$$

From eq. (13), it is clear that only the Pauli terms with $J_{\mathbf{a}} \neq 0$ contribute to the target Hamiltonian H_T . Therefore, we define $\text{nz}(\mathbf{J}) := \{ \mathbf{a} \in \mathbb{F}_2^{2n} \setminus \{\mathbf{0}\} \mid J_{\mathbf{a}} \neq 0 \}$, and require that the Pauli coefficients satisfy

$$\text{nz}(\mathbf{A}) \subseteq \text{nz}(\mathbf{J}). \quad (14)$$

This requirement can be eliminated with single-qubit Clifford conjugation, which we will discuss in detail in section 3.2. In addition to the restriction $\mathbf{a} \in \text{nz}(\mathbf{J})$, given by the system Hamiltonian, we

can also consider a restricted set of conjugation Pauli strings $\mathbf{b} \in \mathcal{F} \subseteq \mathbb{F}_2^{2n}$. However, $\mathcal{F} \subseteq \mathbb{F}_2^{2n}$ has to be chosen such that there still exists a solution. Then, the restricted eq. (13) can be reformulated as

$$A_{\mathbf{a}} = J_{\mathbf{a}} \sum_{\mathbf{b} \in \mathcal{F}} W_{\mathbf{a}\mathbf{b}}^{(r \times s)} \lambda_{\mathbf{b}} \quad \forall \mathbf{a} \in \text{nz}(\mathbf{J}), \quad (15)$$

with the number of non-zero Pauli coefficients $r := |\text{nz}(\mathbf{J})|$ and $s = |\mathcal{F}|$. This can be written as constraints in (LP) $\mathbf{A} = \mathbf{J} \odot (W^{(r \times s)} \boldsymbol{\lambda})$, with the element-wise multiplication \odot and $\mathbf{A}, \mathbf{J} \in \mathbb{R}^r$ restricted to $\mathbf{a} \in \text{nz}(\mathbf{J})$. For the convenience of the following analysis, we define $\mathbf{M} := \mathbf{A} \oslash \mathbf{J}$, with the element-wise division $(\mathbf{A} \oslash \mathbf{J})_{\mathbf{a}} := A_{\mathbf{a}}/J_{\mathbf{a}}$ for all $\mathbf{a} \in \text{nz}(\mathbf{J})$. With that, we define the following LP

$$\begin{aligned} & \text{minimize} && \mathbf{1}^T \boldsymbol{\lambda} \\ & \text{subject to} && W^{(r \times s)} \boldsymbol{\lambda} = \mathbf{M}, \quad \boldsymbol{\lambda} \in \mathbb{R}_{\geq 0}^s. \end{aligned} \quad (\text{PauliLP})$$

The size, and therefore the runtime, of an LP is given by the number of constraints r and the number of variables s . In the case of the partial Walsh-Hadamard matrix, we have $s \leq 4^n$ and $r = |\text{nz}(\mathbf{J})| \leq 4^n - 1$. In section 3.1.2, we propose a simple and efficient relaxation of (PauliLP) where $s \geq 2r$ can be chosen for an arbitrary $r = |\text{nz}(\mathbf{J})|$. This relaxation still leads to an exact decomposition; however, $\mathbf{1}^T \boldsymbol{\lambda}$ is not minimal anymore.

3.1.1 Properties of solutions

In this section, we show the existence of solutions, lower and upper bounds, and worst-case solutions. First, we show that (PauliLP) has a feasible solution for arbitrary Hamiltonians H_S and H_T , satisfying $\text{nz}(\mathbf{A}) \subseteq \text{nz}(\mathbf{J})$, which is a consequence of proposition 3.4.

Corollary 3.5 (existence of solutions). *Let*

$$H_S = \sum_{\mathbf{a} \in \mathbb{F}_2^{2n} \setminus \{\mathbf{0}\}} J_{\mathbf{a}} P_{\mathbf{a}} \quad \text{and} \quad H_T = \sum_{\mathbf{a} \in \mathbb{F}_2^{2n} \setminus \{\mathbf{0}\}} A_{\mathbf{a}} P_{\mathbf{a}}, \quad (16)$$

with $\text{nz}(\mathbf{A}) \subseteq \text{nz}(\mathbf{J})$. Then the partial Walsh-Hadamard matrix $W^{(r \times 4^n)}$ with $r = |\text{nz}(\mathbf{J})|$ leads to a feasible (PauliLP).

Proof. We know that all rows of the Walsh-Hadamard matrix are linearly independent. Furthermore, each row of the Walsh-Hadamard matrix sums to zero, thus $\mathbf{x} = \mathbf{1} > \mathbf{0}$ is a solution to $W^{(r \times 4^n)} \mathbf{x} = \mathbf{0}$. By proposition 3.4 we know that (PauliLP) always has a feasible solution even if we consider an arbitrary subset of rows. \square

To bound the optimal solutions $\mathbf{1}^T \boldsymbol{\lambda}^*$ of (PauliLP) we have to define the dual LP

$$\begin{aligned} & \text{maximize} && \mathbf{M}^T \mathbf{y} \\ & \text{subject to} && (W^{(r \times 4^n)})^T \mathbf{y} \leq \mathbf{1}, \quad \mathbf{y} \in \mathbb{R}^r. \end{aligned} \quad (17)$$

Theorem 3.6 (bounds on solutions). *The optimal objective function value of (PauliLP) with a partial Walsh-Hadamard matrix $W^{(r \times 4^n)}$ is bounded by*

$$\|\mathbf{M}\|_{\ell_{\infty}} \leq \mathbf{1}^T \boldsymbol{\lambda}^* \leq \|\mathbf{M}\|_{\ell_1}. \quad (18)$$

Proof. The lower bound can be verified by the fact that $W^{(r \times 4^n)}$ in (PauliLP) only has entries ± 1 and that $\boldsymbol{\lambda}^*$ is non-negative. Thus, it holds that $\|\mathbf{M}\|_{\ell_{\infty}} = \|W^{(r \times 4^n)} \boldsymbol{\lambda}^*\|_{\ell_{\infty}} \leq \mathbf{1}^T \boldsymbol{\lambda}^*$.

To show the upper bound, we first define the set of feasible solutions for the dual LP (17)

$$\mathcal{F} := \left\{ \mathbf{y} \in \mathbb{R}^r \mid (W^{(r \times 4^n)})^T \mathbf{y} \leq \mathbf{1} \right\}. \quad (19)$$

Next, consider the partial Walsh-Hadamard matrix $W^{((4^n-1) \times 4^n)}$ without the first row, corresponding to the identity Pauli term $P_{\mathbf{a}} = I^{\otimes n}$ with $\mathbf{a} = \mathbf{0}$. We show that

$$\mathcal{S} := \left\{ \mathbf{y} \in \mathbb{R}^{4^n-1} \mid (W^{((4^n-1) \times 4^n)})^T \mathbf{y} \leq \mathbf{1} \right\} \quad (20)$$

is a simplex. A simplex is formed by affine independent vectors. Vectors of the form $(\mathbf{1}, \mathbf{v}_i)^T$ are linearly dependent if and only if the vectors \mathbf{v}_i are affine dependent. From linear dependence it follows that there is a vector $\mathbf{t} \neq \mathbf{0}$ such that $\sum_i t_i (\mathbf{1}, \mathbf{v}_i)^T = \mathbf{0}$. Thus $\sum_i t_i = 0$ and $\sum_i \mathbf{v}_i = \mathbf{0}$, and the vectors \mathbf{v}_i are affine dependent. For any n , the Walsh-Hadamard matrix $W = (\mathbf{1}, (W^{((4^n-1) \times 4^n)})^T)$ has linearly independent rows and columns. Therefore, $W^{((4^n-1) \times 4^n)}$ has affine independent columns, and \mathcal{S} forms a simplex. With $\mathcal{H} = \{\mathbf{y} \in \mathbb{R}^{4^n-1} \mid \|\mathbf{y}\|_{\ell_\infty} \leq 1\}$ we denote the $4^n - 1$ dimensional hypercube. Note that the rows of $W^{(r \times 4^n)}$ are rows of the $4^n \times 4^n$ dimensional Walsh-Hadamard matrix. We define the embedding $g : \mathbb{R}^r \rightarrow \mathbb{R}^{(4^n)-1}$ by appending zeros, such that $(W^{(r \times 4^n)})^T \mathbf{y} = (W^{((4^n-1) \times 4^n)})^T g(\mathbf{y})$. Therefore the objective value of the dual LP (17) can be upper bounded as follows

$$\begin{aligned} \max_{\mathbf{y} \in \mathcal{F}} \langle \mathbf{M}, \mathbf{y} \rangle &= \max_{g(\mathbf{y}) \in \mathcal{S}} \langle g(\mathbf{M}), g(\mathbf{y}) \rangle \\ &\leq \max_{\mathbf{x} \in \mathcal{S}} \langle g(\mathbf{M}), \mathbf{x} \rangle \\ &\leq \max_{\mathbf{x} \in \mathcal{H}} \langle g(\mathbf{M}), \mathbf{x} \rangle = \|\mathbf{M}\|_{\ell_1}. \end{aligned} \quad (21)$$

The upper bound for $\mathbf{1}^T \boldsymbol{\lambda}^*$ follows by strong duality. \square

Next, we show a (not complete) set of instances of (PauliLP), yielding solutions $\boldsymbol{\lambda}^*$ which satisfy the upper bound of theorem 3.6. Such \mathbf{M} constitute the worst cases.

Proposition 3.7. *If $\mathbf{M} \in \{-\mathbf{w}_i \mid \mathbf{w}_i \text{ is the } i\text{-th column of } W^{((4^n-1) \times 4^n)}\}$, then $\mathbf{1}^T \boldsymbol{\lambda}^* = \|\mathbf{M}\|_{\ell_1}$.*

Proof. Let $\mathbf{y} = -\mathbf{w}_i$ be a negative column of $W^{((4^n-1) \times 4^n)}$. Then, by orthogonality of the rows/columns of the Walsh-Hadamard matrix, we obtain

$$\left((W^{((4^n-1) \times 4^n)})^T (-\mathbf{w}_i) \right)_j = \begin{cases} -(4^n - 1), & i = j \\ 1, & \text{otherwise.} \end{cases} \quad (22)$$

Therefore, $\mathbf{y} = -\mathbf{w}_i$ is a feasible solution $(W^{((4^n-1) \times 4^n)})^T \mathbf{y} \leq \mathbf{1}$ to the dual LP (17). The dual objective function value is $\mathbf{M}^T \mathbf{y} = \|\mathbf{w}_i\|_{\ell_1} = 4^n - 1$. Next, we show a feasible solution of (PauliLP). For a $\mathbf{M} = -\mathbf{w}_i$ define

$$\lambda_j = \begin{cases} 0, & i = j \\ 1, & \text{otherwise.} \end{cases} \quad (23)$$

Clearly, this satisfies $W^{((4^n-1) \times 4^n)} \boldsymbol{\lambda} = -\mathbf{w}_i$. Furthermore, the primal objective function value $\mathbf{1}^T \boldsymbol{\lambda} = 4^n - 1$ is the same as for the dual objective function value, which shows optimality. It is easy to see that $\|\mathbf{M}\|_{\ell_1} = 4^n - 1$. \square

3.1.2 Efficient relaxation

We provide an efficient method to construct a feasible matrix $W^{(r \times s)}$ with r rows and $s \geq 2r$ columns, where $r = |\text{nz}(\mathbf{J})|$. The construction is rather simple and consists of sampling uniformly s vectors $\mathbf{b} \in \mathbb{F}_2^{2n}$, where the entries of $W^{(r \times s)}$ are given by the Pauli commutation relation $W_{\mathbf{a}\mathbf{b}}^{(r \times s)} = (-1)^{\langle \mathbf{a}, \mathbf{b} \rangle}$ with $\mathbf{a} \in \text{nz}(\mathbf{J})$. Thus, engineering a Hamiltonian with a Pauli decomposition with r non-zero terms leads to a (PauliLP), with a linear scaling of the number of constraints and variables with r . In previous sections, we proposed sufficient conditions such that the matrix $W \in \mathbb{R}^{r \times s}$ in the (LP) is feasible. This condition is equivalent to $\text{conv}(W)$ having a non-empty interior and $\mathbf{0} \in \text{conv}(W)$.

First, we state general results for i.i.d. copies $\mathbf{x}_1, \dots, \mathbf{x}_s$ of a random vector \mathbf{x} . Then, we relate the results to the partial Walsh-Hadamard matrix $W^{(r \times s)}$ from section 3.1. In the following, we assume that s is large enough and that $\mathbf{x}_1, \dots, \mathbf{x}_s$ are in general position such that $\text{conv}(\mathbf{x}_1, \dots, \mathbf{x}_s)$ always has non-empty interior. Thus, we focus on the condition $\mathbf{0} \in \text{conv}(\mathbf{x}_1, \dots, \mathbf{x}_s)$.

Definition 3.8. *Let $\mathbf{x}_1, \dots, \mathbf{x}_s$ be i.i.d. copies of the arbitrary random vector \mathbf{x} in \mathbb{R}^r and define*

$$p_{s, \mathbf{x}} := \mathbb{P}(\mathbf{0} \in \text{conv}(\mathbf{x}_1, \dots, \mathbf{x}_s)). \quad (24)$$

Lemma 3.9 ([30], Proposition 4). *Let $\mathbf{x} \in \mathbb{R}^r$ be an arbitrary random vector with $\mathbb{E}[\mathbf{x}] = 0$ and $\mathbb{P}(\mathbf{x} \neq 0) > 0$. Then it satisfies*

$$0 < p_{r+1,\mathbf{x}} < p_{r+2,\mathbf{x}} < \cdots < p_{n,\mathbf{x}} < \cdots \rightarrow 1, \quad (25)$$

and $p_{s,\mathbf{x}} = 0$ if $s \leq r$.

This shows strict monotonicity of $p_{(\cdot),\mathbf{x}}$.

Relation to Wendel’s theorem: A well-known related result is Wendel’s theorem [31]: If the random vector in definition 3.8 is spherically symmetric around $\mathbf{0}$ then the probability (24) is given by

$$p_{s,\mathbf{x}} = 1 - \frac{1}{2^{s-1}} \sum_{k=0}^{r-1} \binom{s-1}{k}. \quad (26)$$

This distribution shows a sharp transition from ≈ 0 to ≈ 1 at $s = 2r$. It has been shown that Wendel’s theorem poses an upper bound on $p_{s,\mathbf{x}}$ for absolutely continuous distribution [32] and for arbitrary distributions [30]. We cannot apply Wendel’s theorem to $W^{(r \times s)}$ with randomly sampled columns $\mathbf{b} \stackrel{\text{i.i.d.}}{\sim} \text{unif}(\mathbb{F}_2^{2^n})$ since we do not have a spherical symmetric distribution; see appendix A for details. However, in numerics we will show that random columns of $W^{(r \times 4^n)}$ still show a similar behaviour.

Let \mathbf{w} be a r -dimensional random vector drawn uniformly from $\text{col}(W^{(r \times 4^n)})$. Since $W^{(r \times 4^n)}$ is a partial Walsh-Hadamard matrix with all columns, we can verify $\mathbb{E}[\mathbf{w}] = 0$ and by lemma 3.9 we know that $p_{(\cdot),\mathbf{w}}$ is strictly increasing. We observe a sharp transition of $p_{s,\mathbf{w}}$ at the same position as for spherical symmetric distributions, approximating the upper bound given by Wendel’s theorem. In this sense, $p_{s,\mathbf{w}}$ is optimal, maximizing the success probability for finding a feasible $W^{(r \times s)}$.

Numerical Observation 3.10. *Let $W^{(r \times 4^n)}$ be a partial Walsh-Hadamard matrix with $r = |\text{nz}(\mathbf{J})|$, and let \mathbf{w} be a r -dimensional random vector drawn uniformly from $\text{col}(W^{(r \times 4^n)})$. Then, in figure 1, we observe that Wendel’s statement (26) approximately holds.*

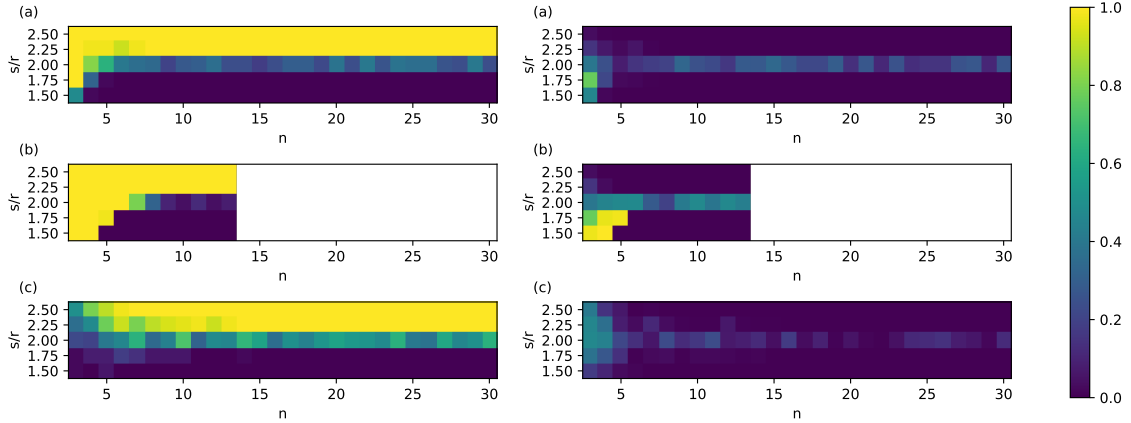


Figure 1: Select r rows of the Walsh-Hadamard matrix $W^{(r \times 4^n)}$, then randomly sample s columns to obtain $W^{(r \times s)}$. **(a)** and **(b)**: The r rows are selected to represent k -local Hamiltonians for $k \leq 2$ and $k \leq 3$ respectively, resulting in $r = \sum_{i=1}^k 3^i \binom{n}{i}$. **(b)**: We stopped the numerical experiments at $n = 13$ due to the large amount of all-to-all interactions with support $k \leq 3$. **(c)**: Sample uniformly random $r = n^2$ rows, representing random Hamiltonians with r non-zero Pauli terms. **Left**: The plots show the success frequency over 50 samples for “ $W^{(r \times s)}$ is feasible” (yellow) for each $n = 3, \dots, 30$ and $s/r = 1.5, \dots, 2.5$. There is a sharp transition at $s/r = 2$ in all cases. **Right**: The difference of our numerical observation from Wendel’s statement (26).

Let $W^{(r \times s)}$ be a partial Walsh-Hadamard matrix with entries $W_{\mathbf{a}\mathbf{b}}^{(r \times s)} = (-1)^{\langle \mathbf{a}, \mathbf{b} \rangle}$ for arbitrary $\mathbf{a} \in \mathbb{F}_2^{2n} \setminus \{\mathbf{0}\}$ and randomly sampled $\mathbf{b} \stackrel{\text{i.i.d.}}{\sim} \text{unif}(\mathbb{F}_2^{2n})$. From numerical Observation 3.10 we know, that such a $W^{(r \times s)}$ is feasible with high probability if $s \geq 2r$ is large enough. This $W^{(r \times s)}$ can be used in (PauliLP) to engineer any Hamiltonian with a Pauli decomposition consisting of r terms. The target Hamiltonian is still decomposed exactly with the efficient relaxation, but $\mathbf{1}^T \boldsymbol{\lambda}$ is no longer minimal. The construction of $W^{(r \times s)}$ is independent of the choice of $\mathbf{a} \in \mathbb{F}_2^{2n} \setminus \{\mathbf{0}\}$. Therefore, one feasible $W^{(r \times s)}$ is also feasible for engineering any Hamiltonian with a Pauli decomposition with r terms with high probability. From the definition of feasibility, we know that (PauliLP) always has a solution for arbitrary \mathbf{M} , i.e. arbitrary \mathbf{J} and \mathbf{A} such that $\text{nz}(\mathbf{A}) \subseteq \text{nz}(\mathbf{J})$.

Furthermore, the quality of the relaxation can be improved by increasing s , which leads to an expanded search space, see figure 2. This provides a flexible trade-off between the runtime of (PauliLP) and the optimality of $\boldsymbol{\lambda}$. The number of interactions r in figure 2 grows quadratic for (a) and (c) and even cubic for (b) with the number of qubits n . However, $\sum \lambda = \mathbf{1}^T \boldsymbol{\lambda}$ grows only linear with n .

All LP's in our work are modelled with the Python package CVXPY [33, 34] and solved with the MOSEK solver [35] on a workstation with 130 GB RAM and the AMD Ryzen Threadripper PRO 3975WX 32-Cores processor. Furthermore, we made the code to reproduce all figures in this work publicly available on GitHub [36].

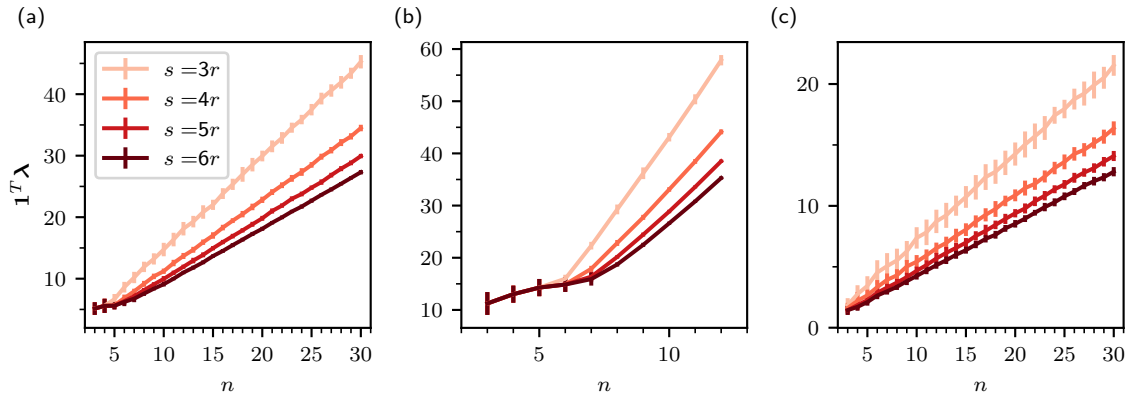


Figure 2: Solving (PauliLP) for 50 uniform random samples $\mathbf{M} = \mathbf{A} \otimes \mathbf{J}$ from $[-1, 1]^r$. For each sample a feasible $W^{(r \times s)}$ is generated as in numerical Observation 3.10 with $s = 3r, \dots, 6r$. The average objective function value $\sum \lambda = \mathbf{1}^T \boldsymbol{\lambda}$ over the number of qubits n is shown. The error bars represent the sample standard deviation. The r interactions of the plots (a), (b) and (c) are chosen the same way as in figure 1.

3.2 Clifford conjugation

In section 3.1, we introduced the Hamiltonian engineering method based on conjugation with Pauli gates. In this section, we extend this method to a certain set of single-qubit Clifford gates. This extension allows us to engineer arbitrary target Hamiltonians which are only restricted by the locality of the Pauli terms in the system Hamiltonian. The same restriction also holds for conjugation with arbitrary single-qubit gates, making Clifford conjugation a powerful Hamiltonian engineering method. The simplest set of single-qubit Clifford gates with full expressivity are the square-root Pauli gates ($\frac{\pi}{2}$ rotations)

$$\sqrt{X} = \frac{1}{2} \begin{pmatrix} 1+i & 1-i \\ 1-i & 1+i \end{pmatrix}, \quad \sqrt{Y} = \frac{1}{2} \begin{pmatrix} 1+i & -1-i \\ 1+i & 1+i \end{pmatrix}, \quad \sqrt{Z} = \begin{pmatrix} 1 & 0 \\ 0 & i \end{pmatrix}. \quad (27)$$

$S^\dagger P S$	\sqrt{X}	\sqrt{Y}	\sqrt{Z}	\sqrt{X}^\dagger	\sqrt{Y}^\dagger	\sqrt{Z}^\dagger
X	X	Z	$-Y$	X	$-Z$	Y
Y	$-Z$	Y	X	Z	Y	$-X$
Z	Y	$-X$	Z	$-Y$	X	Z

Table 1: Conjugation of Pauli gates $P \in \mathbb{P}$ with square-root Pauli gates $S \in \{\sqrt{X}, \sqrt{Y}, \sqrt{Z}, \sqrt{X}^\dagger, \sqrt{Y}^\dagger, \sqrt{Z}^\dagger\}$.

As displayed in table 1, the conjugation of a Pauli gate with a square-root Pauli gate does not only flip the sign but also changes the interaction type (rotation axis). The change of the interaction type increases the set of Hamiltonians reachable by Clifford conjugation compared to the Pauli conjugation. However, we would like a gate set with properties similar to the conjugation with Pauli gates. To this end, we define and investigate the gate set

$$\mathcal{C}_{XY} := \{Z\} \cup \left\{ QD \mid Q, D \in \{\sqrt{X}, \sqrt{Y}, \sqrt{X}^\dagger, \sqrt{Y}^\dagger\} \right\}, \quad (28)$$

where \mathcal{C}_{ZY} and \mathcal{C}_{XZ} can be defined in a similar fashion. W.l.o.g. we only consider the \mathcal{C}_{XY} gate set. Conjugation of Pauli terms with the Clifford gates $\sqrt{X}\sqrt{Y}$ or $\sqrt{Y}^\dagger\sqrt{X}^\dagger$ changes the interaction type and leaves the sign of the Pauli coefficient unchanged. The signs of the conjugated Pauli terms depend on the rotation direction, i.e. the placement of “ \dagger ”, of the square-root Pauli gates; see table 2 for examples. Therefore, we label an element in \mathcal{C}_{XY} by $c := (p, \mathbf{b}) \in \mathbb{F}_3 \times \mathbb{F}_2^2$, where $p \in \mathbb{F}_3$ represents the changes in the interaction type and $\mathbf{b} \in \mathbb{F}_2^2$ captures the sign flips similar to the Pauli conjugation. Denote $\mathcal{C}_{XY}^{\otimes n}$ a string of single-qubit gates on n qubits from the gate set \mathcal{C}_{XY} . We label each $S_c \in \mathcal{C}_{XY}^{\otimes n}$ with $\mathbf{c} = (c_1, \dots, c_n) = (\mathbf{p}, \mathbf{b}) \in \mathbb{F}_3^n \times \mathbb{F}_2^{2n}$, where $c_i \in \mathbb{F}_3 \times \mathbb{F}_2^2$ represents the single-qubit Clifford gate from \mathcal{C}_{XY} on the i -th qubit. In table 2, we show the effect of conjugating a Pauli gate $P_{\mathbf{a}} \in \mathbb{P}$ with $S_c \in \mathcal{C}_{XY}$.

\mathbf{c}		\mathbf{a}		$(0,0)$	$(1,0)$	$(1,1)$	$(0,1)$
		(a_x, a_z)	$S_c \backslash P_{\mathbf{a}}$				
p	\mathbf{b}	S_c	$P_{\mathbf{a}}$	I	X	Y	Z
0	$(0,0)$	I	I	I	X	Y	Z
	$(1,0)$	X	X	I	X	$-Y$	$-Z$
	$(1,1)$	Y	Y	I	$-X$	Y	$-Z$
	$(0,1)$	Z	Z	I	$-X$	$-Y$	Z
1	$(0,0)$	$\sqrt{X}\sqrt{Y}$	I	I	Z	X	Y
	$(1,0)$	$\sqrt{X}^\dagger\sqrt{Y}$	X	I	Z	$-X$	$-Y$
	$(1,1)$	$\sqrt{X}^\dagger\sqrt{Y}^\dagger$	Y	I	$-Z$	X	$-Y$
	$(0,1)$	$\sqrt{X}\sqrt{Y}^\dagger$	Z	I	$-Z$	$-X$	Y
2	$(0,0)$	$\sqrt{Y}^\dagger\sqrt{X}^\dagger$	I	I	Y	Z	X
	$(1,0)$	$\sqrt{Y}\sqrt{X}$	X	I	Y	$-Z$	$-X$
	$(1,1)$	$\sqrt{Y}\sqrt{X}^\dagger$	Y	I	$-Y$	Z	$-X$
	$(0,1)$	$\sqrt{Y}^\dagger\sqrt{X}$	Z	I	$-Y$	$-Z$	X

Table 2: The coloured cells show the conjugated Pauli gates $S_c^\dagger P_{\mathbf{a}} S_c$ for $P_{\mathbf{a}} \in \mathbb{P}$ conjugated by the single-qubit Clifford gate $S_c \in \mathcal{C}_{XY}$. We label an element in \mathcal{C}_{XY} by $c := (p, \mathbf{b}) \in \mathbb{F}_3 \times \mathbb{F}_2^2$, where $p \in \mathbb{F}_3$ captures the permutation of the conjugated Pauli terms, and \mathbf{b} captures the sign flips similar to the Pauli conjugation. The same relation holds for the gate sets \mathcal{C}_{ZY} and \mathcal{C}_{XZ} , but with modified assignments of c to the single-qubit gates. This can be easily verified with table 1.

Conjugation of H_S with $S_c \in \mathcal{C}_{XY}^{\otimes n}$ leads to

$$S_c^\dagger H_S S_c = \sum_{\mathbf{a} \in \mathbb{F}_2^{2n} \setminus \{0\}} J_{\mathbf{a}} S_c^\dagger P_{\mathbf{a}} S_c = \sum_{\mathbf{a} \in \mathbb{F}_2^{2n} \setminus \{0\}} (-1)^{\langle \mathbf{a}, \mathbf{b} \rangle} J_{\pi_{\mathbf{p}}(\mathbf{a})} P_{\mathbf{a}}, \quad (29)$$

with $\mathbf{c} = (\mathbf{p}, \mathbf{b}) \in \mathbb{F}_3^n \times \mathbb{F}_2^{2n}$ and the permutation $\pi_{\mathbf{p}} : \mathbb{F}_2^{2n} \rightarrow \mathbb{F}_2^{2n}$ with $\pi_{\mathbf{p}}(\mathbf{a}) := (\pi_{p_1}(a_1), \dots, \pi_{p_n}(a_n))$

given by the local permutations $\pi_0, \pi_1, \pi_2 : \mathbb{F}_2^2 \rightarrow \mathbb{F}_2^2$ in the two-line notation

$$\begin{aligned}\pi_0 &:= \begin{pmatrix} (0,0) & (1,0) & (1,1) & (0,1) \\ (0,0) & (1,0) & (1,1) & (0,1) \end{pmatrix}, & \pi_1 &:= \begin{pmatrix} (0,0) & (1,0) & (1,1) & (0,1) \\ (0,0) & (1,1) & (0,1) & (1,0) \end{pmatrix}, \\ \pi_2 &:= \begin{pmatrix} (0,0) & (1,0) & (1,1) & (0,1) \\ (0,0) & (0,1) & (1,0) & (1,1) \end{pmatrix}.\end{aligned}\quad (30)$$

We want to find a decomposition of H_T with $\lambda_c \geq 0$ such that

$$H_T = \sum_{\mathbf{a} \in \mathbb{F}_2^{2n} \setminus \{\mathbf{0}\}} A_{\mathbf{a}} P_{\mathbf{a}} = \sum_{\mathbf{c} \in \mathbb{F}_3^n \times \mathbb{F}_2^{2n}} \lambda_{\mathbf{c}} S_{\mathbf{c}}^\dagger H_S S_{\mathbf{c}}. \quad (31)$$

We define the matrix $W(\mathbf{J}) \in \mathbb{R}^{(4^n - 1) \times 12^n}$ with entries

$$W(\mathbf{J})_{\mathbf{a}\mathbf{c}} := (-1)^{\langle \mathbf{a}, \mathbf{b} \rangle} J_{\pi_{\mathbf{p}}(\mathbf{a})}, \quad (32)$$

for $\mathbf{a} \in \mathbb{F}_2^{2n} \setminus \{\mathbf{0}\}$, excluding the identity term $P_{\mathbf{a}} = I^{\otimes n}$ with $\mathbf{a} = \mathbf{0}$, and $\mathbf{c} \in \mathbb{F}_3^n \times \mathbb{F}_2^{2n}$. Similar to the Pauli conjugation we define the submatrix $W(\mathbf{J})^{(r \times s)} \in \mathbb{R}^{r \times s}$ with entries given in eq. (32) for r row-indices $\mathbf{a} \in \mathbb{F}_2^{2n} \setminus \{\mathbf{0}\}$ and s column-indices $\mathbf{c} \in \mathbb{F}_3^n \times \mathbb{F}_2^{2n}$. The dimensions of the submatrix are kept visible in our notation since r and s will be parameters in the subsequent section. Up to the permutation of \mathbf{J} , the same Walsh-Hadamard matrix structure as in $W^{(r \times s)}$ from section 3.1 is present in $W(\mathbf{J})^{(r \times s)}$. In terms of the matrix $W(\mathbf{J})$ it follows that

$$H_T = \sum_{\mathbf{a} \in \mathbb{F}_2^{2n} \setminus \{\mathbf{0}\}} \sum_{\mathbf{c} \in \mathbb{F}_3^n \times \mathbb{F}_2^{2n}} \lambda_{\mathbf{c}} W(\mathbf{J})_{\mathbf{a}\mathbf{c}} P_{\mathbf{a}}. \quad (33)$$

Due to the permutation in eq. (32) we are no longer restricted by the non-zero coefficients as in the Pauli conjugation. From eq. (33) it follows that for each $A_{\mathbf{a}} \neq 0$ there has to be at least one $J_{\hat{\mathbf{a}}} \neq 0$ such that $\text{supp}(\hat{\mathbf{a}}) = \text{supp}(\mathbf{a})$. Therefore, we define

$$\text{suppnz}(\mathbf{J}) := \{\mathbf{a} \in \mathbb{F}_2^{2n} \setminus \{\mathbf{0}\} \mid \exists \hat{\mathbf{a}} \in \text{nz}(\mathbf{J}), \text{supp}(\hat{\mathbf{a}}) = \text{supp}(\mathbf{a})\}, \quad (34)$$

and require that the Pauli coefficients satisfy

$$\text{nz}(\mathbf{A}) \subseteq \text{suppnz}(\mathbf{J}). \quad (35)$$

In physical terms, this means that we are only restricted by the locality of the Pauli terms in H_S and have full flexibility in the kind of interactions and the interaction strength. In addition to the restriction $\mathbf{a} \in \text{suppnz}(\mathbf{J})$, given by the system Hamiltonian, we can also consider a restricted set of conjugating Clifford strings $\mathbf{c} \in \mathcal{F} \subseteq \mathbb{F}_3^n \times \mathbb{F}_2^{2n}$. However, $\mathcal{F} \subseteq \mathbb{F}_3^n \times \mathbb{F}_2^{2n}$ has to be chosen such that there still exists a solution. Then, the restricted eq. (33) can be reformulated as

$$A_{\mathbf{a}} = \sum_{\mathbf{c} \in \mathcal{F}} W(\mathbf{J})_{\mathbf{a}\mathbf{c}}^{(r \times s)} \lambda_{\mathbf{c}} \quad \forall \mathbf{a} \in \text{suppnz}(\mathbf{J}), \quad (36)$$

with $r := |\text{suppnz}(\mathbf{J})|$ and $s = |\mathcal{F}|$. This can be written as constraints in (LP) $\mathbf{A} = W(\mathbf{J})^{(r \times s)} \boldsymbol{\lambda}$, with $\mathbf{A}, \mathbf{J} \in \mathbb{R}^r$ restricted to $\mathbf{a} \in \text{suppnz}(\mathbf{J})$. With that, we define the following LP

$$\begin{aligned}\text{minimize} & \quad \mathbf{1}^T \boldsymbol{\lambda} \\ \text{subject to} & \quad W(\mathbf{J})^{(r \times s)} \boldsymbol{\lambda} = \mathbf{A}, \quad \boldsymbol{\lambda} \in \mathbb{R}_{\geq 0}^s.\end{aligned}\quad (\text{CliffLP})$$

There always exists a feasible solution of (CliffLP) with $W(\mathbf{J})^{(r \times 12^n)}$, which follows from corollary 3.5 and the Walsh-Hadamard structure in $W(\mathbf{J})^{(r \times 12^n)}$, similar to the Pauli conjugation. In general, we have $s \leq 12^n$ and $r \leq 4^n - 1$. In the next section, we propose a simple and efficient relaxation of (CliffLP), where $s \geq 2r$ can be chosen for arbitrary $r = |\text{suppnz}(\mathbf{J})|$.

3.2.1 Efficient relaxation

The size of (Clifflp) might scale as $O(12^n)$. Therefore, a relaxation is necessary to solve this LP practically. We find an efficient method to construct a feasible matrix $W(\mathbf{J})^{(r \times s)}$ with $r = |\text{suppnz}(\mathbf{J})|$ rows and $s \geq 2r$ columns. Therefore, the relaxation for the Clifford conjugation method has the same scaling as for the Pauli conjugation method. The construction is rather simple and consists of sampling uniformly s vectors $\mathbf{c} \in \mathbb{F}_3^n \times \mathbb{F}_2^{2n}$, where the entries of $W(\mathbf{J})^{(r \times s)}$ can be efficiently calculated with eq. (32). We test again the feasibility conditions of proposition 3.4: $\text{conv}(W(\mathbf{J})^{(r \times s)})$ has a non-empty interior and $\mathbf{0} \in \text{conv}(W(\mathbf{J})^{(r \times s)})$.

Numerical Observation 3.11. *Let $W(\mathbf{J})^{(r \times 12^n)}$ be a matrix with $r = |\text{suppnz}(\mathbf{J})|$ and entries as in eq. (32), and let \mathbf{w} be a r -dimensional random vector drawn uniformly from $\text{col}(W(\mathbf{J})^{(r \times 12^n)})$. Then, in figure 3, we observe that Wendel's statement (26) approximately holds.*

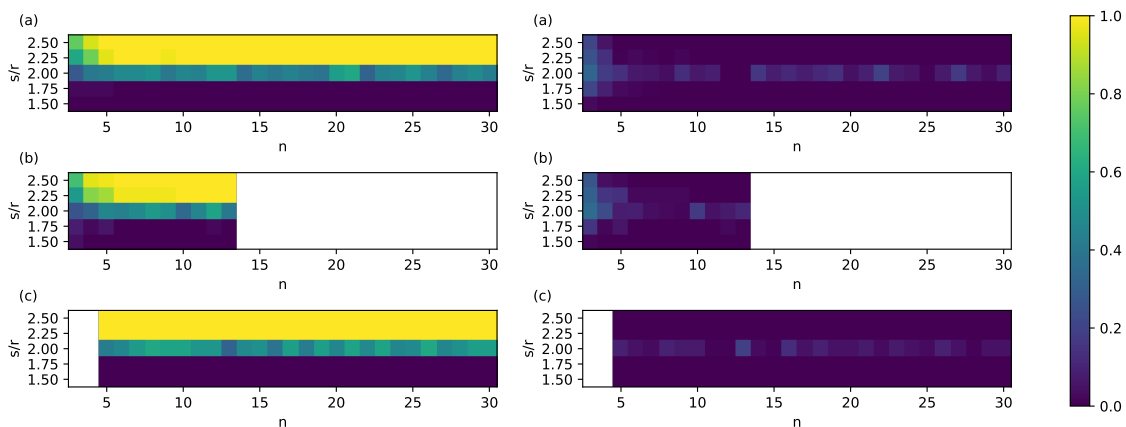


Figure 3: Select r rows of $W(\mathbf{J})$ to get the partial matrix $W(\mathbf{J})^{(r \times 12^n)}$, then randomly sample s columns to obtain $W(\mathbf{J})^{(r \times s)}$. **(a)** and **(b)**: The r rows are selected to represent k -local Hamiltonians for $k \leq 2$ and $k \leq 3$ respectively, resulting in $r = \sum_{i=1}^k 3^i \binom{n}{i}$. **(b)**: We stopped the numerical experiments at $n = 13$ due to the large amount of all-to-all interactions with support $k \leq 3$. **(c)**: For each $k = 1, \dots, 5$ choose randomly 10 different supports $\text{supp}(a)$ and consider all possible interactions on these supports. This results in $r \leq 10 \sum_{k=1}^5 3^k$ ("≤", since for $k = 1$ there are only n different supports). This represents a sparse random 5-local Hamiltonian. **(a)**, **(b)**, **(c)**: For each support, one non-zero value (index a is chosen randomly) is sampled $J_a \stackrel{\text{i.i.d.}}{\sim} \text{unif}([-1, +1])$. At random indices a additional non-zero values are sampled $J_a \stackrel{\text{i.i.d.}}{\sim} \text{unif}([-1, +1])$, otherwise $J_a = 0$. The amount, index, and values of the non-zeros in \mathbf{J} are random. **Left**: The plots show the success frequency over 50 samples for " $W(\mathbf{J})^{(r \times s)}$ is feasible" (yellow) for each $n = 3, \dots, 30$ and $s/r = 1.5, \dots, 2.5$. There is a sharp transition at $s/r = 2$ in all cases. **Right**: The difference of our numerical observation from Wendel's statement (26).

From the definition of feasibility, we know that (Clifflp) always has a solution for arbitrary \mathbf{A} , i.e. arbitrary \mathbf{J}, \mathbf{A} such that $\text{nz}(\mathbf{A}) \subseteq \text{suppnz}(\mathbf{J})$. Furthermore, the quality of the relaxation can be improved by increasing s , which leads to an expanded search space, see figure 4. This provides a flexible trade-off between the runtime of (Clifflp) and the optimality of $\boldsymbol{\lambda}$. The scaling of $\mathbf{1}^T \boldsymbol{\lambda}$ in figure 4 (c) is independent of n since $r \leq 10 \sum_{k=1}^5 3^k$ is independent of n . For the Clifford conjugation, the sample standard deviation is larger compared to the Pauli conjugation. This is due to the increased set of target Hamiltonians which are reachable by the Clifford conjugation. Here, we also randomly sample the number and the position of the non-zero values in \mathbf{J} .

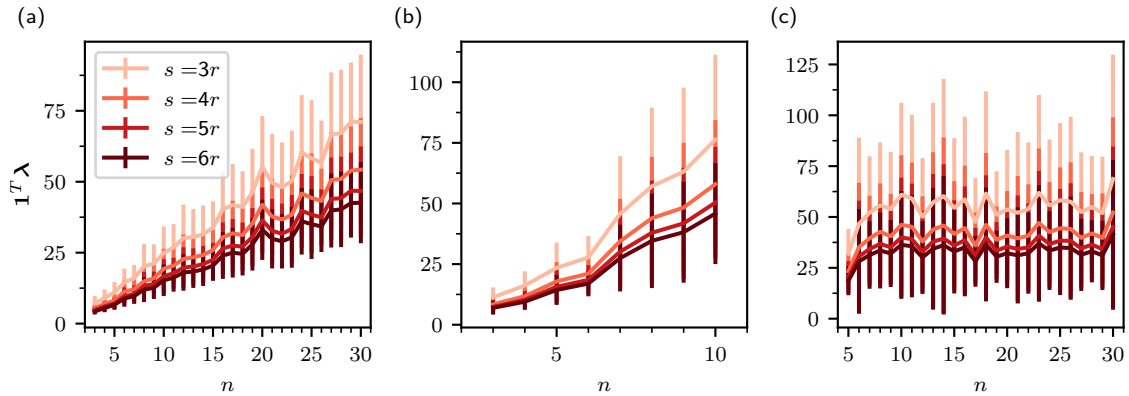


Figure 4: Solving (CliffLP) for 50 uniform random samples \mathbf{A} from $[-1, 1]^r$. For each sample a feasible $W(\mathbf{J})^{(r \times s)}$ is generated as in numerical Observation 3.11 with $s = 3r, \dots, 6r$. The average objective function value $\sum \lambda = \mathbf{1}^T \lambda$ over the number of qubits n is shown. The error bars represent the sample standard deviation. The r interactions and \mathbf{J} of the plots (a), (b) and (c) are chosen the same way as in figure 3.

3.3 Hamiltonian engineering with unknown Hamiltonians

In practice, sometimes not all coupling coefficients in \mathbf{J} might be known. For example, when an experiment aims to realize two-body interactions but also acquires unwanted three-body terms of unknown strength. Such system Hamiltonians with unknown or only partially known coupling strengths can still be engineered using the Pauli conjugation method from section 3.1. Solving (PauliLP) for an $\mathbf{M} \in \mathbb{R}^r$ yields the target Hamiltonian

$$\sum_{\mathbf{a} \in \mathbb{F}_2^{2n} \setminus \{\mathbf{0}\}} M_{\mathbf{a}} J_{\mathbf{a}} P_{\mathbf{a}} = H_T. \quad (37)$$

The potentially unknown coefficients $J_{\mathbf{a}}$ are modified by an element-wise multiplication $\mathbf{M} \odot \mathbf{J}$. Interesting choices for $M_{\mathbf{a}}$ are -1 and 0 , inverting the sign of or canceling the term $P_{\mathbf{a}}$, respectively, without the knowledge of $J_{\mathbf{a}}$. For each term in the system Hamiltonian, a different $M_{\mathbf{a}}$ can be chosen. Therefore, engineering known terms $M_{\mathbf{a}} = A_{\mathbf{a}}/J_{\mathbf{a}}$ in the Hamiltonian while canceling or inverting other (potentially unknown) terms $M_{\mathbf{a}} = 0$ or $M_{\mathbf{a}} = -1$ is possible.

3.4 Hamiltonian engineering with 2D lattice Hamiltonian

The scaling of our method is independent of the system size and only depends on the number of interactions. To highlight this fact, we consider a system Hamiltonian with a 2D square lattice interaction graph. Our Hamiltonian with constant couplings between neighbouring qubits is motivated by experimental quantum platforms such as interacting superconducting qubits or cold atoms in optical lattices [37–39].

We consider a system and target Hamiltonian

$$H_S = \sum_{\mathbf{a} \in \mathbb{F}_2^{2n} \setminus \{\mathbf{0}\}} J_{\mathbf{a}} P_{\mathbf{a}}, \quad H_T = \sum_{\mathbf{a} \in \mathbb{F}_2^{2n} \setminus \{\mathbf{0}\}} A_{\mathbf{a}} P_{\mathbf{a}}, \quad \text{with } \text{supp}(\mathbf{a}) \in E, \quad (38)$$

representing all possible two-body interactions on a 2D square lattice interaction graph with the set of edges E .

Figure 5 shows that a target Hamiltonian H_T with arbitrary couplings \mathbf{A} with this interaction graph can be engineered for 225 qubits in about 60 seconds of classical runtime.

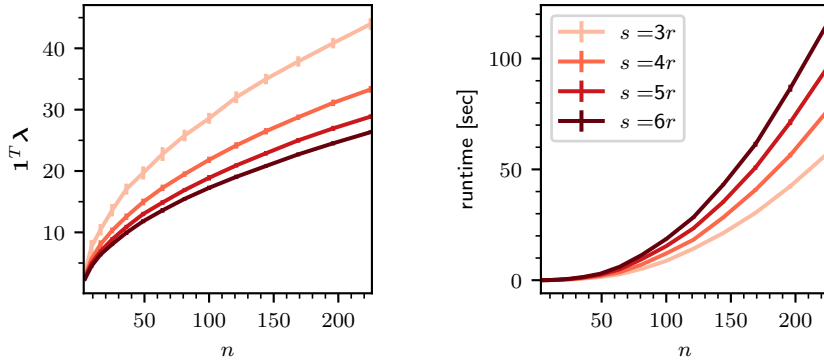


Figure 5: A two-body system Hamiltonian on a 2D square lattice with $n = 4, \dots, 225$ qubits as in eq. (38) and a constant $\mathbf{J} = \mathbf{1}$. The number of interactions is $r = 3^2|E|$ with the set of edges E of a 2D square lattice. We sample 50 target Hamiltonians with uniform random samples \mathbf{A} from $[-1, 1]^r$. For each sample, a feasible $W^{(r \times s)}$ is generated with $s = 3r, \dots, 6r$, using the efficient method from section 3.1.2. **Left:** The average and the sample standard deviation of the objective function value $\sum \lambda = \mathbf{1}^T \boldsymbol{\lambda}$ over the number of qubits n is shown. **Right:** The average and the sample standard deviation of the runtime for solving (PauliLP) over the number of qubits n is shown.

4 Numerical simulations and error considerations

In this section, we provide numerical simulations of our methods under simple but realistic physical error models. In our simulations, we model an ion trap platform with always-on Ising interactions and all-to-all connectivity. We consider two types of error sources: the effect of a finite pulse time and the calibration error of the coupling strength of the system Hamiltonian. For the implementation of non-commuting interactions we additionally investigate the Trotter error.

4.1 Finite pulse time effects.

One potential source of error in our Hamiltonian engineering method is the effect of a finite pulse times, where the system Hamiltonian H_S is also present during the single-qubit pulses. Other errors during the single-qubit gates can be reduced by replacing them with robust composite pulses at the cost of a larger finite pulse time [40–42]. Ideally, we would like to implement

$$e^{i\mathbf{S}} e^{-it\lambda H_S} e^{-i\mathbf{S}}, \quad (39)$$

with the system Hamiltonian H_S and the *relative evolution time* λ . However, the interactions in some platforms are governed by an always-on Hamiltonian H_S , which yields the evolution

$$e^{-itH_{\text{eff}}} = e^{-i(-\mathbf{S}+t_p H_S)} e^{-it\lambda H_S} e^{-i(\mathbf{S}+t_p H_S)}, \quad (40)$$

with the finite pulse duration $0 < t_p$. The term $t_p H_S$ in the exponent can be treated as a small perturbation of the ideal evolution only if $t_p \|\mathbf{J}\|_{\ell_\infty}$ is small. This condition means that the single-qubit gates must be much “faster” than the other interactions in the system. We can express H_{eff} in more detail utilizing the first-order Taylor expansions of the product in eq. (40). Since λ as a solution of the LP is minimized, and t_p is small we can collect the terms with $O(t_p \lambda)$ and treat them as higher order error terms.

$$H_{\text{eff}} = \lambda \mathbf{S}^\dagger H_S \mathbf{S} + \frac{1}{t} (t_p R + O(t_p^2) + O(t_p \lambda)), \quad (41)$$

with

$$R = i \left(\sum_{k=1}^{\infty} \frac{(-i)^k A_k}{k!} \right) e^{i\mathbf{S}} - i e^{-i\mathbf{S}} \left(\sum_{k=1}^{\infty} \frac{(i)^k A_k}{k!} \right), \text{ and with } A_k = \sum_{j=0}^{k-1} \mathbf{S}^{k-1-j} H_S \mathbf{S}^j. \quad (42)$$

The first term in eq. (41) is the ideal implementation. One might hope that the first-order error term R can be mitigated by modifying the constraints in our LP. However, the Pauli terms R do not preserve the locality of the Pauli terms in the system Hamiltonian H_S , a requirement of our Hamiltonian engineering method. Therefore, other compensation mitigation schemes for the finite pulse time error have to be found.

The ideal evolution eq. (39) implies that the interactions governed by the system Hamiltonian H_S can be switched off during the single-qubit pulses. The time dependence of a time independent Hamiltonian being switched on/off can be modeled with a time dependent envelope function $s : \mathbb{R}_{\geq 0} \rightarrow \mathbb{R}_{\geq 0}$. This yields a effective time evolution $e^{-is(t)\tilde{\lambda}H_S}$ with a modified relative evolution time $\tilde{\lambda}$, which has to satisfy

$$t\lambda = \tilde{\lambda} \int_0^t s(t)dt, \quad (43)$$

to implement the desired time evolution $e^{-it\lambda H_S}$.

Another method to compensate the finite pulse time error might be a different scheduling of the single-qubit pulses. Equation (40) reads as follows: trigger the single-qubit pulses, after time t_p wait for time $t\lambda$ then trigger the inverse single-qubit pulses. This results in the total evolution time $2t_p + t\lambda$. A different schedule might be to trigger the single-qubit pulses, and at the same time “start” the waiting time $t\lambda$ then at time $t\lambda - t_p$ trigger the inverse single-qubit pulses. Such a scheme is motivated by the first-order approximation $e^{-i(-S+t_p H_S)} \approx e^{-i(-S)}e^{-it_p H_S}$ given by the Zassenhaus formula [43]. However, the latter scheme performs worse than the former in numerical simulations.

The compensation of the finite pulse time remains an open problem and might be solved by adapting the hardware of quantum devices (to switch on/off H_S) or finding new compensation schemes. For almost all system Hamiltonians in this work, we considered an all-to-all connectivity graph. However, a quantum platform with restricted connectivity such as in section 3.4 reduces the effect of the finite pulse time due to the reduced number of evolution blocks eq. (40). Furthermore, tuning the physical parameters such that $t_p \ll 1/\|\mathbf{J}\|_{\ell_\infty}$ also reduces the finite pulse error as discussed below in section 4.3.

4.2 Hamiltonian simulations

In the following sections, we want to numerically simulate the time evolution of the Pauli and Clifford conjugation methods. To this end, the entire time evolution is simulated as a product of matrix exponentials each approximating the evolution under $\mathbf{S}H_S\mathbf{S}^\dagger$. We split the single-qubit gate pulses into a product of two $\frac{\pi}{2}$ pulses to capture both the Pauli and Clifford conjugation methods. One evolution block consists of a time evolution under the system Hamiltonian conjugated by single-qubit pulses, and has the form

$$U_{\lambda,t_p} := \left(e^{-i(-\mathbf{S}_2+(t_p/2)H_S)} e^{-i(-\mathbf{S}_1+(t_p/2)H_S)} \right) e^{-it\lambda H_S} \left(e^{-i(\mathbf{S}_1+(t_p/2)H_S)} e^{-i(\mathbf{S}_2+(t_p/2)H_S)} \right), \quad (44)$$

with the relative evolution time λ from the (LP) and the $\frac{\pi}{2}$ rotation generators

$$\mathbf{S}_{1/2} = \frac{\pi}{4} \sum_{j=1}^n \pm P^{(j)}, \quad (45)$$

with $P^{(j)} = I^{\otimes j-1} \otimes P \otimes I^{\otimes n-j}$ and $P \in \{I, X, Y, Z\}$. For example, a $(\sqrt{X}\sqrt{Y}^\dagger)^{(1)}$ gate on the first qubit is realized by $S_1 = \frac{\pi}{4}X^{(1)}$ and $S_2 = -\frac{\pi}{4}Y^{(1)}$ and a $X^{(2)}$ gate on the second qubit is realized by $S_1 = S_2 = \frac{\pi}{4}X^{(2)}$. If all $U_{\lambda,0}$ mutually commute, then the total time evolution is given by $U_{\text{sim}} = \prod_{\lambda \neq 0} U_{\lambda,t_p}$. If $U_{\lambda,0}$ are non-commuting, then we use the second-order Trotter formula

$$U_{\text{sim}} = \left(\prod_{\lambda \neq 0}^{\leftarrow} U_{\frac{\lambda}{2c},t_p} \prod_{\lambda \neq 0}^{\rightarrow} U_{\frac{\lambda}{2c},t_p} \right)^c, \quad (46)$$

where the arrows indicate the order of the products and c is the number of cycles, which can be increased to improve the accuracy.

In order to capture the Trotter error, U_{sim} is compared to the target evolution $U_T = e^{-itH_T}$. As a measure of quality, we use the *average gate infidelity*

$$1 - F_{\text{avg}}(U_{\text{sim}}, U_T) = 1 - \frac{\text{Tr}(U_T^\dagger U_{\text{sim}}) + 1}{d + 1}, \quad (47)$$

with the Hilbert space dimension d .

4.3 Simulation with an ion trap model

We consider an ion trap with Ytterbium ions in an external magnetic field gradient [44]. The system Hamiltonian is

$$H_S = - \sum_{i \neq j}^n J_{ij} Z_i Z_j, \quad (48)$$

where the coupling coefficients J_{ij} are calculated for a harmonic trapping potential affecting the equilibrium positions of the ions in the magnetic field gradient. We consider all-to-all connectivity, thus $r = \frac{n}{2}(n-1)$ for the Pauli conjugation and $r = 3^2 \frac{n}{2}(n-1)$ for the Clifford conjugation. The coupling coefficients J_{ij} are proportional to $(B_1/\omega)^2$, with a magnetic field gradient of $B_1 = 40 T/m$ and a trap frequency of $\omega = 2\pi 400 kHz$. We consider the finite pulse time $t_p = \pi/\Omega$, with the Rabi frequency Ω , as a free parameter for now.

4.3.1 Implementing a commuting Hamiltonian

The first target Hamiltonian we consider is

$$H_T = - \sum_{i \neq j}^n A_{ij} Z_i Z_j, \quad (49)$$

with random coupling coefficients $A_{ij} \stackrel{\text{i.i.d.}}{\sim} \text{unif}([0, 1] \cdot Hz)$. We can implement the exact evolution of mutually commuting Hamiltonians. Therefore, we use this as a test bed to investigate the effect of the finite pulse time and calibration errors. We model the calibration errors by a random deviation from the exact value of the coupling coefficients J_{ij} , i.e. $J_{ij}^{err} \stackrel{\text{i.i.d.}}{\sim} J_{ij} \cdot \text{unif}([1 - \varepsilon, 1 + \varepsilon])$ with the error strength ε . To compute the single-qubit pulses and the relative evolution times $\boldsymbol{\lambda}$ we use the Pauli conjugation explained in section 3.1 with $s = 6r = 6(\frac{n}{2}(n-1))$. The effect of the finite pulse time is reduced by combining two Pauli gate layers of adjacent conjugation blocks into one Pauli gate layer, such as

$$\left(\mathbf{S}_1^\dagger e^{-it\lambda_1 H_S} \mathbf{S}_1 \right) \left(\mathbf{S}_2^\dagger e^{-it\lambda_2 H_S} \mathbf{S}_2 \right) = \mathbf{S}_1^\dagger e^{-it\lambda_1 H_S} \mathbf{S}_{12} e^{-it\lambda_2 H_S} \mathbf{S}_2 \quad (50)$$

with $\mathbf{S}_{12} = \mathbf{S}_1 \mathbf{S}_2^\dagger$. The effect of the finite pulse time and the calibration error on the time evolution under the target Hamiltonian in eq. (49) is shown in figure 6. The infidelity due to the finite pulse time seems to be independent from the effective evolution time t , i.e. also independent from any global scaling factor $C > 0$ such that $\boldsymbol{\lambda} \mapsto C\boldsymbol{\lambda}$. This first-order independence can be verified by the finite pulse time error expansion in eq. (41), where the first-order term is independent of t . Contrary to the finite pulse time error, the infidelity due to the calibration error depends on the effective evolution time t . This is expected, since the effective evolution time has a direct effect on the system Hamiltonian coefficients \mathbf{J} . When both errors are present, then the implementation of an Ising Hamiltonian can be achieved with an infidelity below 10^{-3} on 10 qubits, see figure 6 (right).

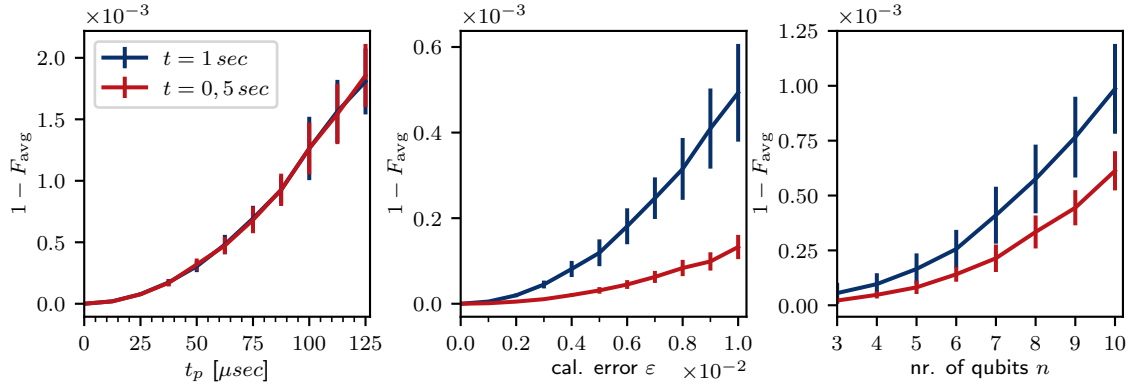


Figure 6: The mean and sample standard deviation of the average gate infidelities eq. (47) for implementing the time evolution of e^{-itH_T} with $t = 1 \text{ sec}$ (blue) and $t = 0.5 \text{ sec}$ (red) and random coupling coefficients $A_{ij} \in [0, 1] \cdot Hz$ is shown. The mean and sample standard deviation are calculated over 50 random samples of Ising Hamiltonians H_T as in eq. (49). For the left & middle plots 10 qubits are considered. **Left:** The infidelity due to the finite pulse time is shown. The finite pulse time causes an infidelity increase with t_p and is independent of the effective evolution time t . **Middle:** The infidelity due to the calibration error is shown. The calibration error is modelled as $J_{ij}^{\text{err}} \stackrel{\text{i.i.d.}}{\sim} J_{ij} \text{unif}(1 - \varepsilon, 1 + \varepsilon]$. Contrary to the finite pulse time error the calibration error depends on the evolution time t , as expected. **Right:** The infidelity due to the finite pulse time and the calibration error over the number of qubits is shown. We chose $t_p = 62.5 \mu\text{sec}$ and $\varepsilon = 10^{-2}$ such that the infidelities of the two error sources is approximately the same in the left & middle plots.

4.3.2 Implementing Heisenberg Hamiltonian

An interesting Hamiltonian due to many applications in physics is the Heisenberg Hamiltonian. However, the Heisenberg Hamiltonian can be challenging to implement. We consider as target the general Heisenberg Hamiltonian

$$H_T = - \sum_{i \neq j}^n (A_{ij}^x X_i X_j + A_{ij}^y Y_i Y_j + A_{ij}^z Z_i Z_j), \quad (51)$$

with coupling coefficients $A_{ij}^x, A_{ij}^y, A_{ij}^z \stackrel{\text{i.i.d.}}{\sim} \text{unif}([0, 1] \cdot Hz)$.

To generate H_T from the Ising Hamiltonian H_S we use the Clifford conjugation explained in section 3.2 with $s = 6r = 6(3^2 \frac{n}{2} (n-1))$. To approximate the time evolution under H_T we use the second-order Trotter formula from eq. (46). Increasing the number of Trotter cycles c improves the accuracy of the Trotter formula in theory. However, an increased number of Trotter cycles c also yields an increased number of evolution blocks U_{λ, t_p} . In the presence of finite pulse times and calibration errors, we investigate the convergence of the second-order Trotter formula to the ideal evolution. For small c , the Trotter error predominates in figure 7. For large c , the finite pulse time error outweighs the calibration and Trotter errors, preventing a simulation with arbitrary precision. If only the calibration error is present, then the Trotter formula converges to a high-fidelity regime similar to the implementation of the mutually commuting Ising Hamiltonian in figure 6. Note that the number of evolution blocks required to achieve a desired accuracy decreases for a reduced effective evolution time t . Thus, even in the presence of the finite pulse time and calibration error, the best possible infidelity is improved. Figure 7 highlights, that practical applications are limited by the effect of the finite pulse time.

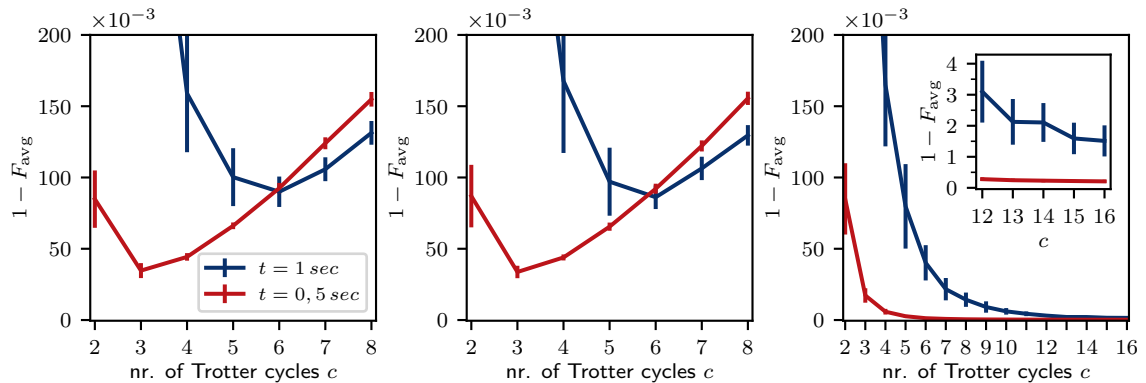


Figure 7: The mean and sample standard deviation of the average gate infidelities eq. (47) for implementing the time evolution of e^{-itH_T} with $t = 1 \text{ sec}$ (blue) and $t = 0,5 \text{ sec}$ (red) and random coupling coefficients $A_{ij}^x, A_{ij}^y, A_{ij}^z \in [0, 1] \cdot \text{Hz}$ over the number of Trotter cycles c is shown. The mean and sample standard deviation are calculated over 50 random samples of the Heisenberg Hamiltonians H_T from eq. (51) on $n = 8$ qubits. **Left:** Implementing the Heisenberg Hamiltonian with a finite pulse time of $t_p = 2,5 \mu\text{sec}$ and a calibration error of $\varepsilon = 10^{-2}$. **Middle:** Implementing the Heisenberg Hamiltonian with a finite pulse time of $t_p = 2,5 \mu\text{sec}$ and no calibration error. **Right:** Implementing the Heisenberg Hamiltonian with a calibration error of $\varepsilon = 10^{-2}$ and no finite pulse time error. The inset shows a zoomed-in version of the right plot.

5 Discussion and outlook

We provide an efficient and flexible method to engineer arbitrary Hamiltonians, requiring only the set of Pauli or single-qubit Clifford gates. Our efficient method is based on solving an LP, and the runtime depends only on the number and locality of Pauli terms in the system Hamiltonian. The Pauli conjugation method is even applicable if only partial knowledge of the system Hamiltonian is available which might be used to cancel unwanted error terms. Our efficient Clifford conjugation method is as powerful (same restrictions) as conjugation with arbitrary single-qubit gates. Moreover, the quality of the solutions can be improved at the cost of a higher runtime, which provides a flexible trade-off. We demonstrate the practicality of our method by simulating physically motivated examples and addressing the most dominant error sources. We discuss in detail the effect of the finite pulse time error and mitigation strategies. However, this error remains an open problem for platforms with always-on interactions. Some platforms like arrays of configurable cold atoms or superconducting qubits offer to some extent the ability to switch on/off the interaction Hamiltonian. This feature can hence be used in experiments to avoid the finite pulse time error. Moreover, a higher-order or randomized product formula can help to reduce the resources to implement the target Hamiltonian and therefore also reduce the effect of errors. The flexibility and efficiency of our methods to engineer arbitrary Hamiltonians might already find many applications in areas within quantum computation and quantum simulation. For example, the fast implementation of multi-qubit gates on devices with arbitrary connectivity or analogue quantum simulation for problems arising in many-body physics. Furthermore, some recent Hamiltonian learning schemes rely on “reshaping” an unknown Hamiltonian to a diagonal Hamiltonian which can be efficiently done with our Pauli conjugation method [45, 46].

In the future, we would like to extend the efficient Hamiltonian engineering method to fermionic systems.

Acknowledgements

We are grateful to Ivan Boldin, Patrick Huber, Markus Nünnerich and Rodolfo Muñoz Rodriguez for fruitful discussions on the ion trap platform. We are also grateful to Matthias Zipper and Christopher Cedzich for fruitful discussions on gate designs for ion trap platforms. Furthermore, we want to thank Özgün Kum for invaluable comments on our manuscript.

This work has been funded by the German Federal Ministry of Education and Research (BMBF) within the funding program “Quantum Technologies – from Basic Research to Market” via the joint project MIQRO (grant number 13N15522) and the Fujitsu Services GmbH as part of an endowed professorship “Quantum Inspired and Quantum Optimization.”

Appendix

A Comments on the efficient relaxation for the Pauli conjugation

As mentioned in the main text, Wendel’s theorem is applicable to spherical symmetric distributions. This would imply that sampling a certain column from $W^{(r \times 4^n)}$ has the same probability as sampling the same column with a flipped sign. Recall that for a partial Walsh-Hadamard matrix $W_{\mathbf{a}\mathbf{b}}^{(r \times 4^n)} = (-1)^{\langle \mathbf{a}, \mathbf{b} \rangle}$, with $\langle \mathbf{a}, \mathbf{b} \rangle = \mathbf{a}_x \cdot \mathbf{b}_z + \mathbf{a}_z \cdot \mathbf{b}_x$. It holds that

$$W_{\mathbf{a}\mathbf{b}}^{(r \times 4^n)} = -W_{\mathbf{a}\bar{\mathbf{b}}}^{(r \times 4^n)} \quad \forall \mathbf{a}, \mathbf{b} \in \mathbb{F}_2^{2n}, \quad (52)$$

for $|a| = 1 \bmod 2$ and with the binary complement $\bar{\mathbf{b}}$ is given element-wise given by $\bar{x} := 1 - x$ for any $x \in \{0, 1\}$. If the decomposition of H_S has only terms $J_{\mathbf{a}} P_{\mathbf{a}}$ with odd $|a|$, then we can apply Wendel’s theorem directly. In this case, we have a success probability of $1/2$ to find a feasible $W^{(r \times 2r)}$ (with r interactions) if we sample $2r$ many $\mathbf{b} \in \mathbb{F}_2^{2n}$ uniformly random. However, an example of such a Hamiltonian with two-body interactions is

$$H = \sum_{i=1}^n (J_i^X X_i + J_i^Y Y_i) + \sum_{i \neq j}^n (J_{ij}^{XZ} X_i Z_j + J_{ij}^{YZ} Y_i Z_j), \quad (53)$$

and with commuting interactions is

$$H = \sum_{i=1}^n J_i^X X_i + \sum_{ijk}^n J_{ijk}^{XXX} X_i X_j X_k, \quad (54)$$

with arbitrary coupling constants. Unfortunately, for a general Hamiltonian, we cannot use Wendel’s theorem to construct a relaxation for (PauliLP).

Recently, lower bounds on $p_{s,\mathbf{x}}$ have been proposed for arbitrary distributions [30]. However, their results rely on the halfspace depth (or Tukey depth), which is hard to compute. It is a measure of how extreme a point is with respect to a distribution of random points.

Definition A.1 (halfspace depth). *Let \mathbf{x} be an arbitrary r -dimensional random vector. Then, the halfspace depth at the origin is defined as*

$$\alpha_{\mathbf{x}} := \inf_{\|\mathbf{c}\|=1} \mathbb{P}(\mathbf{c}^T \mathbf{x} \leq 0). \quad (55)$$

The halfspace depth $\alpha_{\mathbf{x}}$ is the minimum (fraction) number of points in a halfspace with the origin on the boundary.

Theorem A.2 ([30, Theorem 14]). *Let \mathbf{x} be an arbitrary r -dimensional random vector. Then, for each positive integer $s \geq 3r/\alpha_{\mathbf{x}}$, we have*

$$p_{s,\mathbf{x}} > 1 - \frac{1}{2^r}. \quad (56)$$

Let \mathbf{w} be a r -dimensional random vector drawn uniformly from $\text{col}(W^{(r \times 4^n)})$. From corollary 3.5, we find the trivial lower bound $1/4^n \leq \alpha_{\mathbf{w}}$, since at least one point is in an arbitrary halfspace with the origin on its boundary. Finding a constant lower bound $1/\beta \leq \alpha_{\mathbf{w}}$ would imply that for $s \geq 3r\beta$ we find a feasible $W^{(r \times s)}$ with high probability. One needs to show that at least $4^{O(n)}$ points are contained in an arbitrary halfspace with the origin on its boundary.

References

- [1] R. Somma, G. Ortiz, J. E. Gubernatis, E. Knill, and R. Laflamme, *Simulating physical phenomena by quantum networks*, *Phys. Rev. A* **65**, 042323 (2002), [arXiv:quant-ph/0108146](#).
- [2] R. Blatt and C. F. Roos, *Quantum simulations with trapped ions*, *Nat. Phys.* **8**, 277 (2012).
- [3] D. Wecker, M. B. Hastings, N. Wiebe, B. K. Clark, C. Nayak, and M. Troyer, *Solving strongly correlated electron models on a quantum computer*, *Phys. Rev. A* **92**, 062318 (2015), [arXiv:1506.05135](#).
- [4] H. Bernien, S. Schwartz, A. Keesling, H. Levine, A. Omran, H. Pichler, S. Choi, A. S. Zibrov, M. Endres, M. Greiner, V. Vuletić, and M. D. Lukin, *Probing many-body dynamics on a 51-atom quantum simulator*, *Nature* **551**, 579 (2017), [arXiv:1707.04344](#).
- [5] J. Olson, Y. Cao, J. Romero, P. Johnson, P.-L. Dallaire-Demers, N. Sawaya, P. Narang, I. Kivlichan, M. Wasielewski, and A. Aspuru-Guzik, *Quantum information and computation for chemistry*, [arXiv:1706.05413](#) (2017).
- [6] J. Zhang, G. Pagano, P. W. Hess, A. Kyprianidis, P. Becker, H. Kaplan, A. V. Gorshkov, Z.-X. Gong, and C. Monroe, *Observation of a many-body dynamical phase transition with a 53-qubit quantum simulator*, *Nature* **551**, 601 (2017), [arXiv:1708.01044](#).
- [7] A. J. Daley, I. Bloch, C. Kokail, S. Flannigan, N. Pearson, M. Troyer, and P. Zoller, *Practical quantum advantage in quantum simulation*, *Nature* **607**, 667 (2022).
- [8] J. Preskill, *Quantum Computing in the NISQ era and beyond*, *Quantum* **2**, 79 (2018), [arXiv:1801.00862](#).
- [9] R. Trivedi, A. Franco Rubio, and J. I. Cirac, *Quantum advantage and stability to errors in analogue quantum simulators*, *Nature Communications* **15**, 6507 (2024), [arXiv:2212.04924](#).
- [10] D. W. Leung, I. L. Chuang, F. Yamaguchi, and Y. Yamamoto, *Efficient implementation of coupled logic gates for quantum computation*, *Phys. Rev. A* **61**, 042310 (2000), [arXiv:quant-ph/9904100](#).
- [11] D. Leung, *Simulation and reversal of n -qubit Hamiltonians using Hadamard matrices*, *Journal of Modern Optics* **49**, 1199 (2002), [arXiv:quant-ph/0107041](#).
- [12] J. L. Dodd, M. A. Nielsen, M. J. Bremner, and R. T. Thew, *Universal quantum computation and simulation using any entangling Hamiltonian and local unitaries*, *Phys. Rev. A* **65**, 040301 (2002), [arXiv:quant-ph/0106064](#).
- [13] M. A. Nielsen, M. J. Bremner, J. L. Dodd, A. M. Childs, and C. M. Dawson, *Universal simulation of Hamiltonian dynamics for quantum systems with finite-dimensional state spaces*, *Phys. Rev. A* **66**, 022317 (2002), [arXiv:quant-ph/0109064](#).
- [14] M. Garcia-de Andoin, A. Saiz, P. Pérez-Fernández, L. Lamata, I. Oregi, and M. Sanz, *Digital-analog quantum computation with arbitrary two-body Hamiltonians*, *Phys. Rev. Res.* **6**, 013280 (2024), [arXiv:2307.00966](#).
- [15] D. Hayes, S. T. Flammia, and M. J. Biercuk, *Programmable quantum simulation by dynamic Hamiltonian engineering*, *New J. Phys.* **16**, 10.1088/1367-2630/16/8/083027 (2014), [arXiv:1309.6736](#).
- [16] C. Figgatt, A. Ostrander, N. M. Linke, K. A. Landsman, D. Zhu, D. Maslov, and C. Monroe, *Parallel entangling operations on a universal ion-trap quantum computer*, *Nature* **572**, 368 (2019), [arXiv:1810.11948](#).
- [17] Y. Lu, S. Zhang, K. Zhang, W. Chen, Y. Shen, J. Zhang, J.-N. Zhang, and K. Kim, *Global entangling gates on arbitrary ion qubits*, *Nature* **572**, 363 (2019), [arXiv:1901.03508](#).
- [18] N. Grzesiak, R. Blümel, K. Wright, K. M. Beck, N. C. Pisenti, M. Li, V. Chaplin, J. M. Amini, S. Debnath, J.-S. Chen, and Y. Nam, *Efficient arbitrary simultaneously entangling gates on a trapped-ion quantum computer*, *Nat. Commun.* **11**, 2963 (2020), [arXiv:1905.09294](#).
- [19] J. K. Pachos and M. B. Plenio, *Three-spin interactions in optical lattices and criticality in cluster Hamiltonians*, *Phys. Rev. Lett.* **93**, 056402 (2004), [arXiv:quant-ph/0401106](#).
- [20] H. P. Büchler, A. Micheli, and P. Zoller, *Three-body interactions with cold polar molecules*, *Nature Physics* **3**, 726 (2007), [arXiv:cond-mat/0703688](#).
- [21] X. Peng, J. Zhang, J. Du, and D. Suter, *Quantum simulation of a system with competing two- and three-body interactions*, *Phys. Rev. Lett.* **103**, 140501 (2009), [arXiv:0809.0589](#).

- [22] K. Zhang, H. Li, P. Zhang, J. Yuan, J. Chen, W. Ren, Z. Wang, C. Song, D.-W. Wang, H. Wang, S. Zhu, G. S. Agarwal, and M. O. Scully, *Synthesizing five-body interaction in a superconducting quantum circuit*, *Phys. Rev. Lett.* **128**, 190502 (2022), arXiv:2109.00964.
- [23] P. Baßler, M. Zipper, C. Cedzich, M. Heinrich, P. H. Huber, M. Johanning, and M. Kliesch, *Synthesis of and compilation with time-optimal multi-qubit gates*, *Quantum* **7**, 984 (2023), arXiv:2206.06387.
- [24] P. Baßler, M. Heinrich, and M. Kliesch, *Time-optimal multi-qubit gates: Complexity, efficient heuristic and gate-time bounds*, *Quantum* **8**, 1279 (2024), arXiv:2307.11160.
- [25] S. P. Boyd and L. Vandenberghe, *Convex optimization* (Cambridge University Press, Cambridge, UK ; New York, 2004).
- [26] I. Bárány, *A generalization of Carathéodory’s theorem*, *Discrete Mathematics* **40**, 141 (1982).
- [27] D. A. Spielman and S.-H. Teng, *Smoothed analysis of algorithms: Why the simplex algorithm usually takes polynomial time*, *Journal of the ACM* **51**, 385 (2004), arXiv:cs/0111050.
- [28] J. Farkas, *Theorie der einfachen Ungleichungen*, *Journal für die Reine und Angewandte Mathematik* **124**, 1 (1902).
- [29] E. Stiemke, *Über positive Lösungen homogener linearer Gleichungen*, *Mathematische Annalen* **76**, 340 (1915).
- [30] S. Hayakawa, T. Lyons, and H. Oberhauser, *Estimating the probability that a given vector is in the convex hull of a random sample*, *Probability Theory and Related Fields* **185**, 705 (2023), arXiv:2101.04250.
- [31] J. G. Wendel, *A problem in geometric probability.*, *MATHEMATICA SCANDINAVICA* **11**, 109–112 (1962).
- [32] U. Wagner and E. Welzl, *A continuous analogue of the upper bound theorem*, *Discrete & Computational Geometry* **26**, 205 (2001).
- [33] A. Agrawal, R. Verschuere, S. Diamond, and S. Boyd, *A rewriting system for convex optimization problems*, *J. Control Decis.* **5**, 42 (2018), arXiv:1709.04494.
- [34] S. Diamond and S. Boyd, *CVXPY: A Python-embedded modeling language for convex optimization*, *J. Mach. Learn. Res.* **17**, 1 (2016), arXiv:1603.00943.
- [35] MOSEK ApS, *MOSEK Optimizer API for Python 9.3.14* (2022).
- [36] P. Baßler, *Source code for “Efficient Hamiltonian engineering”*, <https://github.com/paba92/EffHamEng> (2024).
- [37] F. Arute et al., *Quantum supremacy using a programmable superconducting processor*, *Nature* **574**, 505 (2019), arXiv:1910.11333.
- [38] L. Schmid, D. F. Locher, M. Rispler, S. Blatt, J. Zeiher, M. Müller, and R. Wille, *Computational capabilities and compiler development for neutral atom quantum processors—connecting tool developers and hardware experts*, *Quantum Sci. Technol.* **9**, 10.1088/2058-9565/ad33ac (2024), arXiv:2309.08656.
- [39] L. Henriët, L. Beguin, A. Signoles, T. Lahaye, A. Browaeys, G.-O. Reymond, and C. Jurczak, *Quantum computing with neutral atoms*, *Quantum* **4**, 327 (2020), arXiv:2006.12326.
- [40] M. A. Ali Ahmed, G. A. Álvarez, and D. Suter, *Robustness of dynamical decoupling sequences*, *Phys. Rev. A* **87**, 042309 (2013), arXiv:1211.5001.
- [41] G. T. Genov, D. Schraft, N. V. Vitanov, and T. Halfmann, *Arbitrarily accurate pulse sequences for robust dynamical decoupling*, *Phys. Rev. Lett.* **118**, 133202 (2017), arXiv:1609.09416.
- [42] H. L. Gevorgyan and N. V. Vitanov, *Ultrahigh-fidelity composite rotational quantum gates*, *Phys. Rev. A* **104**, 012609 (2021), arXiv:2012.14692.
- [43] F. Casas, A. Murua, and M. Nadinic, *Efficient computation of the Zassenhaus formula*, *Computer Physics Communications* **183**, 2386 (2012), arXiv:1204.0389.
- [44] C. Piltz, T. Sriarunothai, S. S. Ivanov, S. Wölk, and C. Wunderlich, *Versatile microwave-driven trapped ion spin system for quantum information processing*, *Sci. Adv.* **2**, e1600093 (2016), arXiv:1509.01478.
- [45] H.-Y. Huang, Y. Tong, D. Fang, and Y. Su, *Learning many-body Hamiltonians with Heisenberg-limited scaling*, *Phys. Rev. Lett.* **130**, 200403 (2023), arXiv:2210.03030.
- [46] M. Ma, S. T. Flammia, J. Preskill, and Y. Tong, *Learning k-body Hamiltonians via compressed sensing*, arXiv:2410.18928 (2024).